The Plant Cell, Vol. 20: 2357–2371, September 2008, www.plantcell.org © 2008 American Society of Plant Biologists

Arabidopsis WRKY38 and WRKY62 Transcription Factors Interact with Histone Deacetylase 19 in Basal Defense [W]

Kang-Chang Kim, Zhibing Lai, Baofang Fan, and Zhixiang Chen[1]

Department of Botany and Plant Pathology, Purdue University, West Lafayette, Indiana 47907-2054

***Arabidopsis thaliana WRKY38* and *WRKY62*, encoding two structurally similar type III WRKY transcription factors, are induced in a Nonexpressor of PR Gene1 (NPR1)–dependent manner by salicylic acid (SA) or by virulent *Pseudomonas syringae*. Disease resistance and SA-regulated *Pathogenesis-Related1* (*PR1*) gene expression are enhanced in the *wrky38* and *wrky62* single mutants and, to a greater extent, in the double mutants. Overexpression of *WRKY38* or *WRKY62* reduces disease resistance and *PR1* expression. Thus, WRKY38 and WRKY62 function additively as negative regulators of plant basal defense. WRKY38 and WRKY62 interact with Histone Deacetylase 19 (HDA19). Expression of *HDA19* is also induced by *P. syringae*, and the stability of its induced transcripts depends on SA and NPR1 in infected plants. Disruption of *HDA19* leads to compromised resistance, whereas its overexpression results in enhanced resistance to *P. syringae*. Thus, HDA19 has a role opposite from those of WRKY38 and WRKY62 in basal resistance to the bacterial pathogen. Both WRKY38 and WRKY62 are transcriptional activators in plant cells, but their activation activities are abolished by overexpressed HDA19. Interaction of WRKY38 and WRKY62 with HDA19 may act to fine-tune plant basal defense responses.**

INTRODUCTION

Detection of an invading pathogen by a plant triggers a complex set of signal transduction pathways and a battery of defense mechanisms. Upon perception of pathogen/microbe-associated molecular patterns (PAMPs), plants can activate distinct mitogen-activated protein kinase cascades, leading to PAMP-triggered immunity (PTI) (Jones and Dangl, 2006). Successful pathogens suppress PTI through secreted effector proteins and, as a result, cause diseases. Coevolution of plant hosts with the virulent pathogens can give rise to specific plant disease resistance (R) proteins that recognize pathogen effectors and activate highly efficient effector-triggered immunity (ETI) (Jones and Dangl, 2006).

Both PTI and ETI are associated with the accumulation of defense signal molecules such as salicylic acid (SA), ethylene (ET), and jasmonic acid (JA). In *Arabidopsis thaliana*, SA-regulated defense responses including *Pathogenesis-Related* (*PR*) gene expression require the function of the *Nonexpressor of PR Gene1* (*NPR1*) gene, which encodes a 66-kD protein with ankyrin repeats (Cao et al., 1997). *Arabidopsis* mutants deficient in SA biosynthesis or signaling are compromised in resistance to biotrophic pathogens that feed on living host tissue during the whole or part of their infection cycle. ET- and JA-mediated signaling pathways, on the other hand, often mediate plant defense against necrotrophic pathogens that promote host cell death at early stages of infection (Glazebrook, 2004). A number of studies have shown that SA and ET/JA signaling pathways are mutually antagonistic (Kunkel and Brooks, 2002). For example, mutations of JA signaling regulators such as COI1 can enhance SA accumulation and signaling in pathogen-infected plants (Kloek et al., 2001), and blocking SA accumulation can promote JA signaling (Spoel et al., 2003). Other studies have shown that SA and ET/JA signaling pathways can interact positively or even synergistically in plant defense responses (Kloek et al., 2001; Mur et al., 2006). It has been suggested that the apparent discrepancy of the relationship between SA and JA signaling may arise from the concentration-specific outcomes of their interactions (Mur et al., 2006). When both signals were applied at low levels, a transient synergistic enhancement was observed in the expression of genes associated with JA or SA. When applied at high levels or at prolonged times, the two signals become antagonistic to each other.

WRKY DNA binding transcription factors play important roles in the regulation of genes associated with plant defense responses (Eulgem and Somssich, 2007). Recent mutant analyses in *Arabidopsis* have revealed direct links between specific WRKY proteins and complex defense responses. *Arabidopsis* WRKY70 has been shown to regulate the crosstalk between SA- and JA-mediated signaling by promoting SA-dependent and suppressing JA-dependent responses (Li et al., 2004, 2006). Mutations of *WRKY70* have been shown to enhance plant susceptibility to both biotrophic and necrotrophic pathogens, including the bacterial pathogen *Erwinia carotovora*, as well as the fungal pathogens *Erysiphe cichoracearum* and *Botrytis cinerea* (Li et al., 2004, 2006; AbuQamar et al., 2006). In addition, *wrky70* mutants are compromised in both basal defense and R gene (*RPP4*)–mediated disease resistance to the oomycete *Hyaloperonospora parasitica* (Knoth et al., 2007). By contrast, a number of *Arabidopsis* WRKY proteins, including WRKY7, WRKY11, and WRKY17, function as negative regulators of plant basal defense (Park et al., 2005; Journot-Catalino et al., 2006; Kim et al., 2006). Mutations of these genes enhance basal plant resistance to virulent *Pseudomonas syringae* strains. The structurally related WRKY18, WRKY40, and WRKY60 have partially redundant roles as negative

[1] Address correspondence to zhixiang@purdue.edu.

The author responsible for distribution of materials integral to the findings presented in this article in accordance with the policy described in the Instructions for Authors (www.plantcell.org) is: Zhixiang Chen (zhixiang@purdue.edu).

[W] Online version contains Web-only data.

www.plantcell.org/cgi/doi/10.1105/tpc.107.055566

regulators in plant resistance against the biotrophic bacterial pathogen *P. syringae* and the fungal pathogen *E. cichoracearum* (Xu et al., 2006; Shen et al., 2007). The *wrky18 wrky40* double mutant and the *wrky18 wrky40 wrky60* triple mutant, however, are more susceptible to the necrotrophic fungal pathogen *B. cinerea* (Xu et al., 2006). Thus, these three WRKY proteins appear to be involved in the antagonistic crosstalk of defense mechanisms against different types of microbial pathogens. In a previously reported study, *Arabidopsis* mitogen-activated protein kinase4 (MPK4), an activator of JA/ET-mediated defense and a repressor of SA-dependent resistance (Petersen et al., 2000), was found to interact with the MPK4 substrate MKS1, which, in turn, interacts with *Arabidopsis* WRKY25 and WRKY33 (Andreasson et al., 2005). In addition, WRKY25 and WRKY33 are phosphorylated by MPK4 in vitro, and a *wrky33* knockout mutant expresses elevated levels of *PR1* under short-day growth conditions (Andreasson et al., 2005). Disruption of *WRKY33* results in enhanced susceptibility to necrotrophic fungal pathogens and impaired expression of JA/ET-regulated defense genes (Zheng et al., 2006). These results indicate that WRKY33 functions as a positive regulator of JA/ET-mediated pathways and plays an important role in disease resistance to necrotrophic fungal pathogens. Although the *wrky33* mutants respond normally to *P. syringae*, mutations of *WRKY25* enhance tolerance to the bacterial pathogen (Zheng et al., 2007). In addition, overexpression of either *WRKY25* or *WRKY33* enhances susceptibility to the bacterial pathogen and suppresses SA-regulated *PR1* gene expression (Zheng et al., 2006, 2007). These results suggest that WRKY25 and WRKY33 function as downstream components of the MPK4-mediated SA-repressing and JA/ET-activating signaling pathways. Thus, WRKY transcription factors play diverse roles in plant defense responses. These diverse roles of WRKY proteins may reflect the complex signaling and transcriptional networks of plant defense through the actions of a wide range of interactive positive and negative regulators.

Arabidopsis WRKY38 and WRKY62, encoding two structurally related type III WRKY transcription factors, are induced by both pathogen infection and SA treatment (Yu et al., 2001; Dong et al., 2003; Kalde et al., 2003; Mao et al., 2007). In this study, we report that WRKY38 and WRKY62 function additively as negative regulators of plant basal defense. WRKY38 and WRKY62 interact in the nucleus with Histone Deacetylase 19 (HDA19), which functions as a positive regulator of plant basal disease resistance. Both WRKY38 and WRKY62 activate transcription in plant cells, but this activity can be abolished by overexpressed HDA19. Thus, the physical interactions provide a specific mechanism for the functional antagonism of the defense-repressing WRKY transcriptional activators for the defense-activating HDA19 transcriptional repressor that may function in the tight regulation and fine-tuning of plant defense responses.

RESULTS

Structures, DNA Binding, and Subcellular Localization of WRKY38 and WRKY62

WRKY proteins can be classified into three groups (Eulgem et al., 2000). The first group contains two Cys_2His_2 zinc-finger motifs, and the second group contains only one Cys_2His_2 zinc-finger motif. The third group of WRKY proteins contains a single $Cys_2HisCys$ motif. Based on this classification, WRKY38 and WRKY62 belong to group III WRKY proteins, each with a single $Cys_2HisCys$ motif (see Supplemental Figure 1A online). Besides the conserved WRKY domains, the two proteins share substantial levels of homology at their N termini, but the sequence similarity at their C termini is relatively low (see Supplemental Figure 1A online).

WRKY transcription factors are thought to function by binding their cognate TTGACC/T W-box *cis* elements in the promoter regions of target genes and activating or repressing their expression (Ulker and Somssich, 2004). A number of isolated WRKY proteins have been shown to bind W-box sequences (Rushton et al., 1996; Chen and Chen, 2000; Yu et al., 2001). To examine the DNA binding activity of WRKY38 and WRKY62, we expressed the genes in *Escherichia coli*, purified the recombinant protein, and assayed their binding to an oligonucleotide that contains a TTGACC W-box sequence (P12a; see Supplemental Figure 1B online) using electrophoretic mobility shift assays. A protein/DNA complex with reduced mobility was detected when purified recombinant WRKY38 or WRKY62 protein was incubated with the P12a probe (see Supplemental Figure 1B online). Binding of the WRKY proteins to a mutant probe (mP12a) in which the TTGACC sequence was changed to TTGAAC was not detectable (see Supplemental Figure 1B online). Thus, binding of WRKY38 and WRKY62 to the TTGACC W-box sequence is highly specific.

To determine the subcellular location of WRKY38 and WRKY62, we constructed green fluorescent protein (GFP) fusions to the C termini of the two WRKY proteins. The fusion constructs, driven by the cauliflower mosaic virus (*CaMV*) *35S* promoter, were directly bombarded into onion (*Allium cepa*) epidermal cells. The transiently expressed WRKY38-GFP and WRKY62-GFP fusion proteins were localized exclusively to the nucleus (see Supplemental Figure 1C online). By contrast, GFP was found in both the nucleus and cytoplasm (see Supplemental Figure 1C online).

SA- and NPR1-Dependent Expression of *WRKY38* and *WRKY62*

To analyze the involvement of WRKY38 and WRKY62 in plant basal defense, we analyzed their expression in response to the virulent *P. syringae* pv *tomato* strain DC3000 (*Pst*DC3000). As shown in Figure 1A, *WRKY38* and *WRKY62* transcripts were undetectable in healthy uninfected plants or in plants infiltrated with 50 mM $MgCl_2$ (mock inoculation). In plants infiltrated with *Pst*DC3000, transcripts for *WRKY38* or *WRKY62* remained undetectable at 4 h after inoculation (HAI) but were elevated at 8 and 12 HAI before declining to almost basal levels by 24 HAI (Figure 1A). To determine the role of SA in pathogen-induced *WRKY38* and *WRKY62* expression, we compared their pathogen-induced expression in wild-type plants with those in the SA signaling–defective *npr1-3* mutant and the *sid2-3* mutant (SALK_133146), which contains a T-DNA insertion in the *SID2* gene important for SA biosynthesis (Cao et al., 1997; Wildermuth et al., 2001). As shown in Figure 1B, transcripts for both *WRKY38*

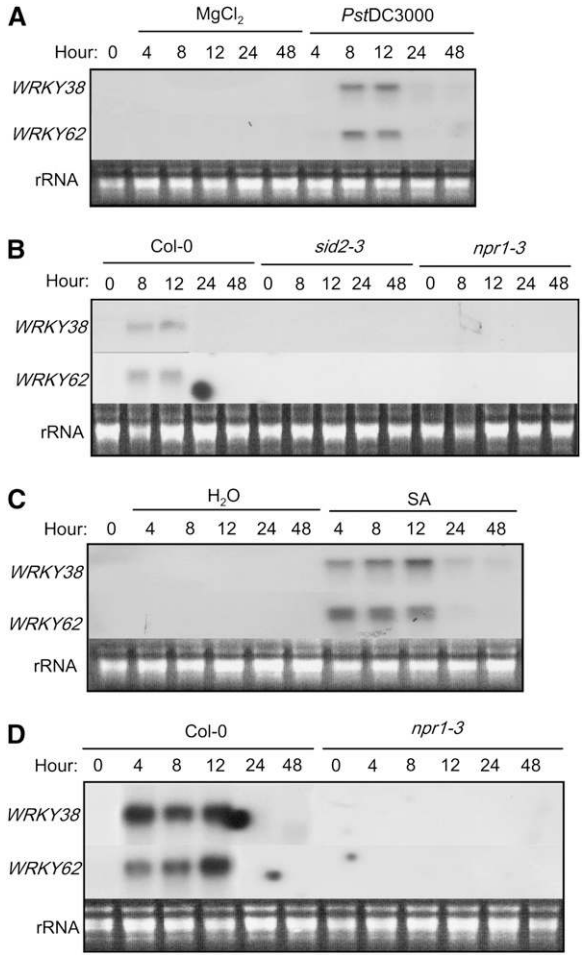

Figure 1. Pathogen- and SA-Induced Expression of *WRKY38* and *WRKY62*.

(A) Time course of pathogen-induced expression of *WRKY38* and *WRKY62*. Five-week-old *Arabidopsis* plants (Col-0) were infiltrated with 10 mM $MgCl_2$ or *Pst*DC3000 (OD_{600} = 0.0001 in 10 mM $MgCl_2$). The infiltrated leaves were collected at the indicated times after inoculation for RNA isolation. RNA gel blot analysis was performed with a ^{32}P-labeled *WRKY38* probe. The blot was stripped and reprobed with the *WRKY62* probe. Ethidium bromide staining of rRNA is shown for the assessment of equal loading.

(B) SA and NPR1 dependence of pathogen-induced expression of *WRKY38* and *WRKY62*. Five-week-old wild-type (Col-0), *npr1-3*, and *sid2-3* mutant plants were infiltrated with *Pst*DC3000. Leaf collection, RNA isolation, and RNA gel blot analysis of *WRKY38* and *WRKY62* expression were performed as in **(A)**.

(C) Time course of SA-induced expression of *WRKY38* and *WRKY62*. Five-week-old *Arabidopsis* plants (Col-0) were sprayed with water or SA (1 mM). Leaf collection, RNA isolation, and RNA gel blot analysis of *WRKY38* and *WRKY62* expression were performed as in **(A)**.

(D) NPR1 dependence of SA-induced expression of *WRKY38* and *WRKY62*. Five-week-old wild-type (Col-0) and *npr1-3* mutant plants were sprayed with 1 mM SA. Leaf collection, RNA isolation, and RNA gel blot analysis of *WRKY38* and *WRKY62* expression were performed as in **(A)**.

These experiments were performed three times with similar results.

and *WRKY62* were elevated at 8 and 12 HAI in pathogen-infected wild-type plants but not in the pathogen-infected *sid2* and *npr1* mutants. Quantitative RT-PCR showed that the levels of WRKY38 and WRKY62 transcripts were elevated 8- to 10-fold at 8 and 12 HAI in wild-type plants but not in the *sid2* and *npr1* mutants (see Supplemental Figure 2 online). Thus, induction of *WRKY38* and *WRKY62* by the virulent bacterial pathogen is dependent on SA and NPR1.

To further determine the involvement of SA in the induction of *WRKY38* and *WRKY62*, we examined their expression in wild-type plants after spraying with water (control) or 1 mM SA. Expression of *WRKY38* and *WRKY62* was induced by SA but not by water (Figure 1C). Unlike in pathogen-inoculated plants, transcripts for both *WRKY38* and *WRKY62* were elevated at 4 h after SA spraying, indicating that SA induces their expression more rapidly than *Pst*DC3000 inoculation. The transcripts for the two WRKY genes remained highly expressed during the following 8 h after SA spraying before declining to near basal levels, as observed in pathogen-inoculated plants (Figure 1C). In the *npr1-3* mutant, SA-induced expression of *WRKY38* and *WRKY62* was completely abolished (Figure 1D). Thus, SA-induced expression of *WRKY38* and *WRKY62* is NPR1-dependent. The expression data suggest that *WRKY38* and *WRKY62* function downstream of *NPR1* in SA-mediated defense signaling pathways.

Disruption of *WRKY38* and *WRKY62* Enhances Plant Basal Defense

To analyze the role of *WRKY38* and *WRKY62* directly, we identified T-DNA insertion or transposon-tagged mutants for both *WRKY38* and *WRKY62*. The *wrky38-1* mutant (WiscDsLox489-492C21; Columbia [Col-0] ecotype) contains a T-DNA insertion in the second intron, while *wrky38-2* (RATM11-6950-1_H; Nossen-0 [No-0] ecotype) contains a *Ds* transposon insertion in the last exon of the *WRKY38* gene (see Supplemental Figure 3A online). The *wrky62-1* (GABI_016H10; Col-0 ecotype) and *wrky62-2* (RATM11-6212-1_G; No-0 ecotype) mutants contain a T-DNA and a *Ds* transposon insertion, respectively, in the second exon of the *WRKY62* gene (see Supplemental Figure 3A online). Homozygous mutant plants were identified by PCR with *WRKY38*- or *WRKY62*-specific primers. RNA gel blot analysis failed to detect *WRKY38* or *WRKY62* transcripts of the expected sizes in the respective homozygous mutants after SA treatment (see Supplemental Figures 3B and 3C online). To determine possible functional redundancy, we also generated the *wrky38-1 wrky62-1* (Col-0 ecotype) and *wrky38-2 wrky62-2* (No-0 ecotype) double mutants through genetic crossing. The *wrky38* and *wrky62* single and double mutants showed no differences in growth, development, or morphology from wild-type plants.

To determine possible changes of the mutants in plant basal disease resistance, we inoculated them with *Pst*DC3000 and monitored both bacterial growth and disease symptom development. As shown in Figures 2A and 2B, the *wrky38* and *wrky62* single mutants had 2.5- to 4-fold reductions in the growth of the bacterial pathogen. The single mutants also developed significantly less severe disease symptoms than wild-type plants after infection (Figures 2C and 2D). A greater reduction (8- to 11-fold) of bacterial growth was observed in the *wrky38 wrky62* double

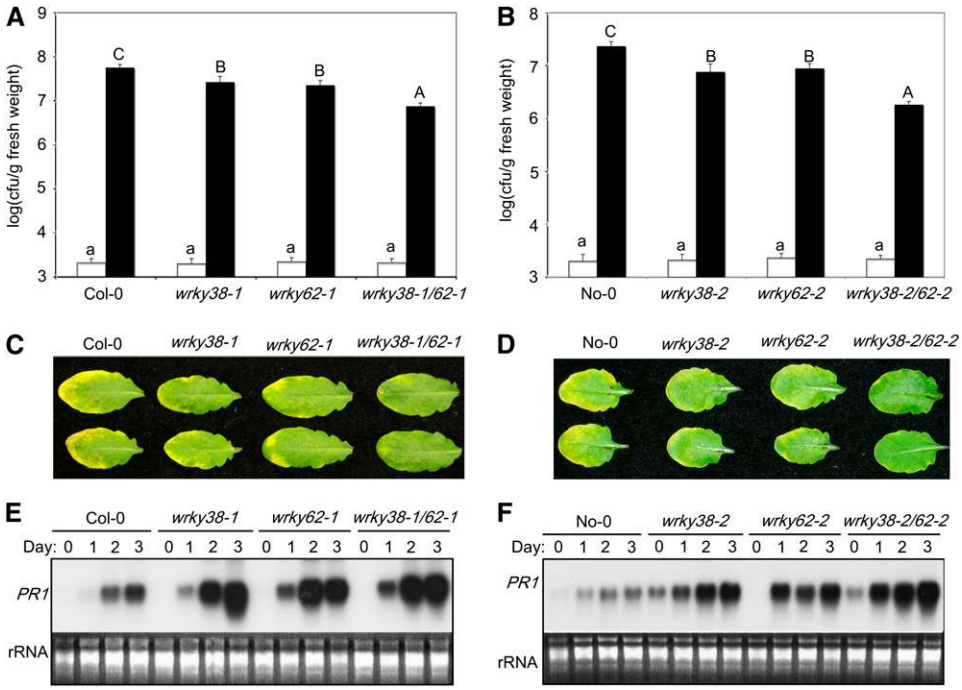

Figure 2. Altered Responses of the WRKY Mutants to *Pst*DC3000.

(A) and **(B)** Altered bacterial growth in the WRKY mutants. Wild type, single mutants, and double mutants for *WRKY38* and *WRKY62* were infiltrated with a suspension of *Pst*DC3000 (OD_{600} = 0.0001 in 10 mM $MgCl_2$). Samples were taken at 0 (open bars) or 3 (closed bars) DAI to determine bacterial growth. Means and SE were calculated from 10 plants for each treatment. According to Duncan's multiple range test (P = 0.05), means of colony-forming units do not differ at 0 DAI significantly if they are indicated with the same lowercase letter and do not differ significantly at 3 DAI if they are indicated with the same uppercase letter.
(C) and **(D)** Altered disease symptom development in the WRKY mutants. Pathogen inoculation of wild-type and mutant plants was performed as in **(A)** and **(B)**. Photographs of pairs of representative inoculated leaves were taken at 4 DAI **(C)** and 5 DAI **(D)**.
(E) and **(F)** Pathogen-induced *PR1* expression. Wild type, single mutants, and double mutants for *WRKY38* and *WRKY62* were infiltrated with a suspension of *Pst*DC3000 (OD_{600} = 0.0001 in 10 mM $MgCl_2$). Inoculated leaves were collected at the indicated DAI for RNA isolation. RNA gel blot analysis was performed with ^{32}P-labeled *PR1*.
These experiments were performed four times with similar results.

mutants relative to that in the wild-type plants (Figures 2A and 2B). The marked reduction in bacterial growth in the double mutants was accompanied by a substantially reduced development of disease symptoms (Figures 2C and 2D). These results suggest that WRKY38 and WRKY62 function additively with a negative role in basal resistance to the virulent bacterial pathogen.

Overexpression of *WRKY38* and *WRKY62* Compromises Plant Basal Defense

To further examine the roles of WRKY38 and WRKY62, we overexpressed the WRKY genes in transgenic *Arabidopsis* plants. Constructs containing a full-length *WRKY38* or *WRKY62* cDNA driven by the *CaMV 35S* promoter were transformed into *Arabidopsis* (Col-0 ecotype), and transgenic plants were identified by selection for antibiotic resistance. RNA gel blotting identified several transgenic plants that contained elevated levels of *WRKY38* or *WRKY62* transcripts even in the absence of SA treatment (see Supplemental Figures 3D and 3E online). Two transgenic lines that constitutively expressed *WRKY38* or *WRKY62* at elevated levels and contained a single T-DNA locus in their genomes, based on the ratio of antibiotic resistance phenotypes in progeny, were chosen for further study.

Constitutive overexpression of a number of *Arabidopsis* WRKY genes, such as *WRKY7* and *WRKY18*, resulted in reduced growth, altered flowering time, and changed leaf morphology (Chen and Chen, 2002; Kim et al., 2006). Analysis of F3 homozygous plants from *WRKY38*- or *WRKY62*-overexpressing transgenic plants revealed no differences in growth, development, or morphology from wild-type plants. Following inoculation with *Pst*DC3000, the transgenic *WRKY38* and *WRKY62* overexpression lines displayed greater bacterial growth (~4- to 6-fold) than wild-type plants (Figure 3A). The inoculated leaves of *WRKY38*- and *WRKY62*-overexpressing plants also developed more severe disease symptoms than those of wild-type plants after infection (Figure 3B). For comparison, the *npr1-3* mutant had ~10-fold higher bacterial growth than wild-type plants and developed even more severe disease symptoms than the *WRKY38*- or *WRKY62*-overexpressing plants (Figures 3A and 3B). These results support the hypothesis that WRKY38 and WRKY62 have negative roles in basal resistance to the bacterial pathogen.

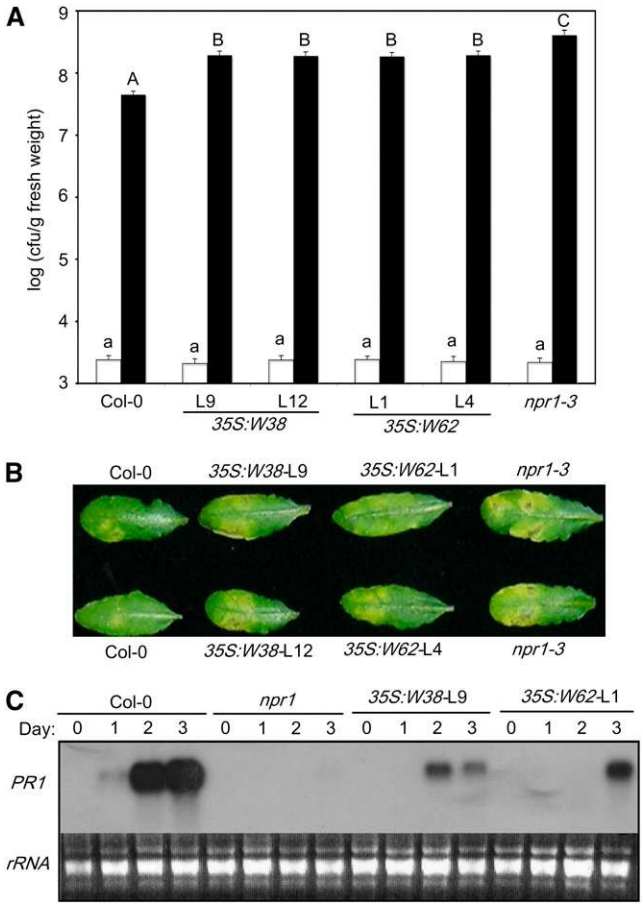

Figure 3. Characterization of *WRKY38* and *WRKY62* Overexpression Lines.

(A) Altered bacterial growth. Wild-type, overexpression line, and *npr1* mutant plants were infiltrated with a suspension of *Pst*DC3000 (OD_{600} = 0.0001 in 10 mM $MgCl_2$). Samples were taken at 0 (open bars) or 3 (closed bars) DAI to determine the growth of the bacterial pathogen. Means and SE were calculated from 10 plants for each treatment. According to Duncan's multiple range test (P = 0.05), means of colony-forming units do not differ significantly at 0 DAI if they are indicated with the same lowercase letter and do not differ significantly at 3 DAI if they are indicated with the same uppercase letter.

(B) Altered disease symptom development. Pathogen inoculation was performed as in **(A)**. Photographs of representative inoculated leaves were taken at 3 DAI.

(C) Pathogen-induced *PR1* expression. Wild-type, overexpression line, and *npr1* mutant plants were infiltrated with a suspension of *Pst*DC3000 (OD_{600} = 0.0001 in 10 mM $MgCl_2$). Inoculated leaves were collected at the indicated DAI for RNA isolation. RNA gel blot analysis was performed with ^{32}P-labeled *PR1*.

These experiments were performed four times with similar results.

Defense Gene Expression

SA plays an important role in *Arabidopsis* resistance to *Pst*DC3000 (Glazebrook, 2004). To investigate how WRKY38 and WRKY62 repress plant basal resistance to *Pst*DC3000, we examined SA-regulated *PR1* expression in both the knockout mutants and overexpression lines following infection of the bacterial pathogen. After *Pst*DC3000 infection, there were higher levels of *PR1* transcripts at 1, 2, and 3 d after inoculation (DAI) in the *wrky38* and *wrky62* mutants than in the wild-type plants. In addition, the *wrky38-1 wrky62-1* double mutant (in Col-0 ecotype) had higher levels of *PR1* transcripts than the *wrky38-1* and *wrky62-2* single mutants in three of the four independent experiments performed, while the *wrky38-2 wrky62-2* double mutant (in No-0 ecotype) had higher levels of *PR1* transcripts than the *wrky38-2* and *wrky62-2* single mutants in all four experiments (Figures 2E and 2F). By contrast, *WRKY38*- and *WRKY62*-overexpressing lines expressed lower levels of *PR1* than wild-type plants after *Pst*DC3000 infection (Figure 3C). Thus, altered resistance to *Pst*DC3000 is correlated with altered expression of SA-regulated *PR1* genes in the mutants and overexpression lines for *WRKY38* and *WRKY62*.

To further investigate the role of WRKY38 and WRKY62 in SA-regulated defense gene expression, we examined the sensitivity of the mutants and overexpression lines to SA for *PR1* expression. The mutant and overexpression plants were sprayed with various concentrations of SA and examined for *PR1* expression 24 h later. As shown in Figure 4, the *wrky38-1* and *wrky62-1* single mutants had slightly higher levels of *PR1* transcripts than wild-type plants, particularly after treatment with relatively higher concentrations (0.5 and 1.0 mM) of SA. The *wrky38-1 wrky62-1* double mutant had substantially higher levels of *PR1* transcripts than wild-type plants at all of the SA concentrations tested (Figure 4). By contrast, the *WRKY38*- and *WRKY62*-overexpressing lines accumulated lower levels of *PR1* transcripts than wild-type plants after treatment of different concentrations of SA (Figure 4). Thus, WRKY38 and WRKY63 negatively regulate plant responsiveness to SA for *PR1* expression.

Physical Interactions of WRKY38 and WRKY62 with HDA19

To study how WRKY38 and WRKY62 repress plant basal defense, we next attempted to isolate their interacting proteins. The commonly used Gal4 two-hybrid system based on interaction-dependent transcriptional activation of reporter genes, however, is not useful because both WRKY38 and WRKY62 act as transcriptional activators in yeast cells (data not shown). Therefore, we used the yeast CytoTrap system based on interaction-dependent activation of the Ras signaling pathway and cell growth in a temperature-sensitive yeast mutant (Broder et al., 1998). The yeast mutant contains a temperature-sensitive mutation in the *cdc25* gene encoding a guanyl nucleotide-exchange factor, which binds and activates Ras. In these screens, we used a fusion protein of WRKY62 with the human homolog of yeast cdc25, hSOS, as bait. The temperature-sensitive yeast strain transformed with the bait construct failed to grow at the restrictive temperature (37°C). We screened >10^7 independent transformants of a cDNA prey library generated from SA-treated *Arabidopsis* plants. The screens yielded one group of cDNAs that all encoded HDA19 (Tian and Chen, 2001; Tian et al., 2003) (see Supplemental Figure 4A online).

We subsequently tested their interactions in plant cells using the bimolecular fluorescence complementation (BiFC) assay in *Agrobacterium tumefaciens*–infiltrated tobacco (*Nicotiana*

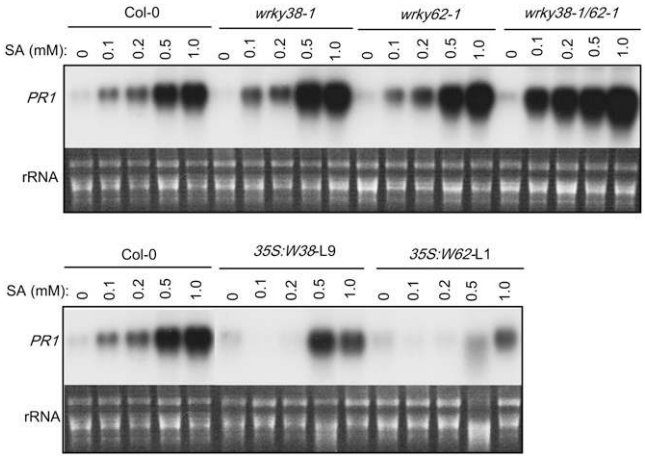

Figure 4. Roles of WRKY38 and WRKY62 in Plant SA Sensitivity for *PR1* Induction.

Five-week-old wild-type (Col-0), knockout mutant, and overexpression plants for *WRKY38* and *WRKY62* were sprayed with SA at the indicated concentrations. Leaf samples were collected at the indicated times after spraying for RNA isolation. RNA gel blot analysis was performed with ^{32}P-labeled *PR1*. These experiments were performed twice with similar results.

benthamiana) leaves (Cui et al., 2007). WRKY62 was fused to the N-terminal yellow fluorescent protein (YFP) fragment and HDA19 was fused to the C-terminal YFP fragment. When WRKY62-N-YFP was coexpressed with HDA19-C-YFP, a strong BiFC signal was observed predominantly in the nuclear compartment, based on staining with 4,6-diamidino-2-phenylindole (DAPI) (Figure 5). Since WRKY38 is structurally and functionally related to WRKY62, we also examined its interaction with HDA19 in plant cells using the BiFC assay. Indeed, when WRKY38 was fused to the terminal YFP fragment and coexpressed with HDA19-C-YFP in tobacco leaves, a BiFC signal was also observed predominantly in the nuclear compartment (Figure 5). Control experiments in which WRKY38-N-YFP or WRKY62-N-YFP was coexpressed with unfused C-YFP protein or unfused N-YFP was coexpressed with HDA19-C-YFP did not show any fluorescence (Figure 5). These experiments provide strong evidence that both WRKY38 and WRKY62 form complexes with HDA19 in the nuclear compartment of plant cells. Interactions of WRKY38 and WRKY62 with HDA19 in the nucleus are consistent with the subcellular localization of WRKY38, WRKY62, and HDA19 in the nuclear compartment (see Supplemental Figure 1C online) (Long et al., 2006).

To determine the specificity of interactions, we analyzed interactions of three other WRKY proteins with HDA19 by BiFC. We fused WRKY48 (a group II WRKY protein) and WRKY70 (a group III WRKY protein) to the N-terminal YFP fragment but found no BiFC signal when the two constructs were coexpressed with HDA19-C-YFP in tobacco leaves (data not shown). We also fused WRKY18 to the N-terminal YFP fragment, coexpressed it with HDA19-C-YFP in tobacco leaves, and again found no BiFC signal (see Supplemental Figure 5 online). We have previously shown that WRKY18 interacts with WRKY40 based on both yeast two-hybrid assays and in vivo immunoprecipitation (Xu et al., 2006). Indeed, when WRKY40 was fused to the C-terminal YFP fragment and coexpressed with WRKY18-N-YFP in tobacco leaves, a strong BiFC signal was observed predominantly in the nuclear compartment (see Supplemental Figure 5 online). To further analyze their interactions in plant cells, we performed coimmunoprecipitation with MYC-HDA19 and FLAG-WRKY38 or FLAG-WRKY62 transiently expressed in tobacco leaves. The protein complexes immunoprecipitated by the anti-MYC antibody from protein extracts of leaves coexpressing MYC-HDA19 and FLAG-WRKY38 or MYC-HDA19 and FLAG-WRKY62 generated positive interactions to the anti-FLAG antisera (see Supplemental Figure 4B online). By contrast, the immunoprecipitation from protein extracts of leaves expressing MYC-HDA19 and FLAG-WRKY18 produced no cross-reactivity to the antisera (see Supplemental Figure 4B online).

Regulated Expression of *HDA19*

As a first step to characterize the role of HDA19 in plant resistance to *Pst*DC3000, we analyzed its expression in wild-type plants after infection of the bacterial pathogen. The *HDA19* transcript levels were very low before inoculation and at 12 HAI (Figure 6A). However, *HDA19* transcripts were readily detected by RNA gel blot analysis in pathogen-inoculated plants at 24 HAI and continued to increase gradually during the next 24 h. No significant induction of *HDA19* was observed in plants infiltrated with $MgCl_2$ (Figure 6A). Thus, expression of *HDA19* is induced by *Pst*DC3000. In addition, transcripts for *HDA19* were elevated in SA- or methyl jasmonate (MeJA)–treated plants (Figure 6B), although the induction was delayed when compared with those of *WRKY38* and *WRKY62* in SA-treated plants (Figure 1A). Pathogen-, SA-, and MeJA-induced expression of *HDA19* was also detected by quantitative RT-PCR (see Supplemental Figure 6 online).

To analyze the signaling pathways that lead to *HDA19* expression, we examined pathogen-induced changes of *HDA19* transcript levels in mutants defective in SA, JA, or ET signaling. In the *sid2-3* and *npr1-3* mutants, defective in SA biosynthesis and signaling, respectively, expression of *HDA19* was still induced, based on increased levels of *HDA19* transcripts (Figure 6C). Interestingly, the induced *HDA19* transcripts were reduced in size, most likely due to increased degradation, although the possibility of alternative degradation cannot be completely ruled out (Figure 6C). In the *coi1-1* and *ein2-1* mutants, there were slightly higher basal levels of *HDA19* transcripts than in wild-type plants in two of the three experiments performed (Figure 6C). After pathogen infection of the mutants, *HDA19* transcripts were also elevated, and the accumulated transcripts appeared to be intact as in the wild-type plants (Figure 6C). Thus, the stability of *HDA19* transcripts accumulated in pathogen-infected plants appears to be dependent on SA signaling.

Knockout Mutant and Overexpression Plants for *HDA19*

To determine its role in plant basal disease resistance, we identified two T-DNA insertion mutants for *HDA19* (*hda19-3* and *hda19-4*) that both contain a T-DNA insertion in the first exon of the gene (see Supplemental Figure 7A online). We inoculated

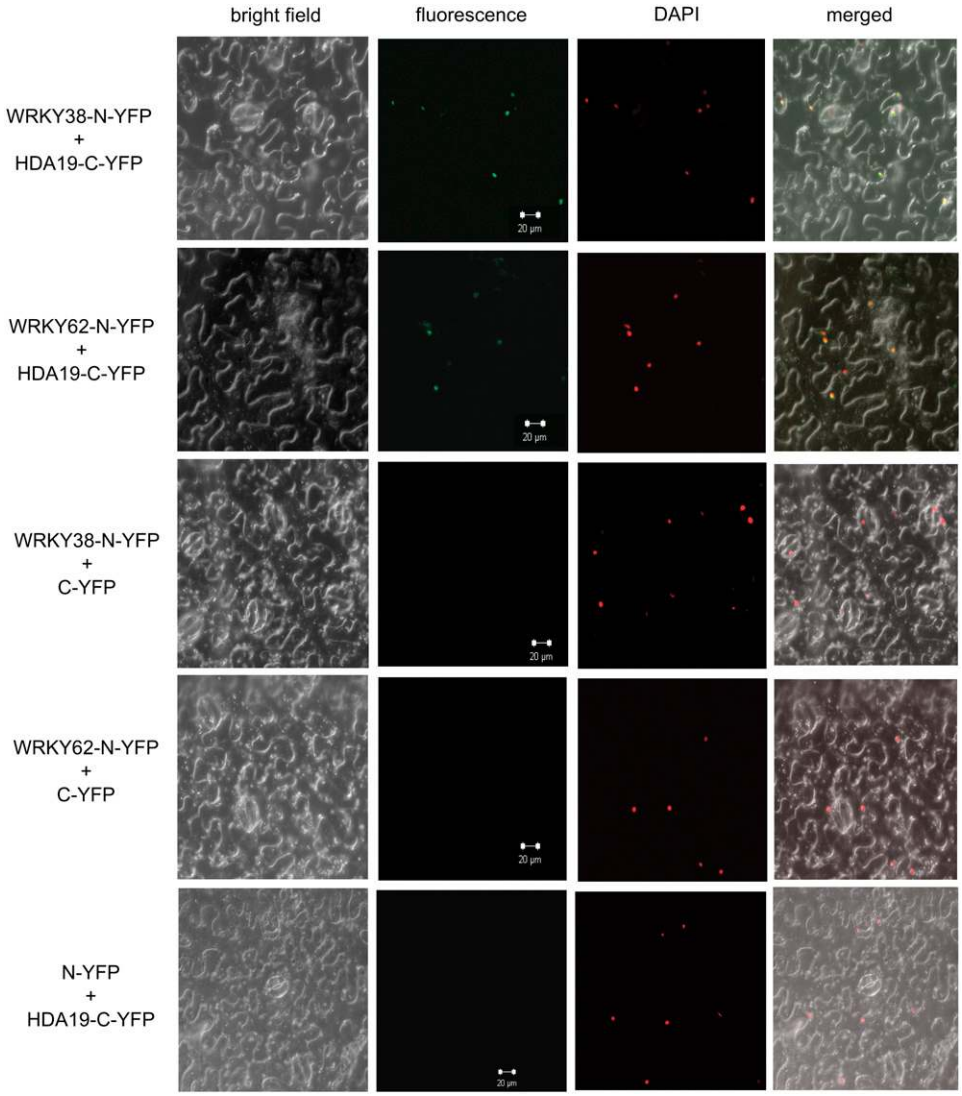

Figure 5. BiFC Analysis of WRKY Protein Interactions with HDA19.

Fluorescence was observed from complementation of the N-terminal part of the YFP fused with WRKY38 (WRKY38-N-YFP) or WRKY62 (WRKY62-N-YFP) with the C-terminal part of the YFP fused with HDA19 (HDA19-C-YFP) and colocalized with DAPI stains in the nuclear compartment of tobacco leaf epidermal cells. No fluorescence was observed when WRKY38-N-YFP or WRKY62-N-YFP was coexpressed with unfused C-YFP or when unfused N-YFP was coexpressed with HDA19-C-YFP. These experiments were performed three times with similar results.

the *hda19* knockout mutant plants with *Pst*DC3000 and monitored both bacterial growth and disease symptom development. As shown in Figure 7A, the *hda19* mutants had an approximately fivefold increase in the growth of the bacterial pathogen. The mutants also developed more severe disease symptoms than wild-type plants after the infection (Figure 7C). Thus, unlike WRKY38 and WRKY62, HDA19 functions as a positive regulator in basal resistance to *Pst*DC3000.

To further examine the roles of *HDA19*, we overexpressed the gene in transgenic *Arabidopsis* plants. A construct containing a full-length *HDA19* cDNA driven by the *CaMV 35S* promoter was transformed into *Arabidopsis* (Col-0 ecotype), and transgenic plants were identified by selection for antibiotic resistance. RNA gel blotting identified transgenic plants that contained elevated levels of *HDA19* transcript even in the absence of pathogen infection (see Supplemental Figure 7B online). Those F1 lines with high levels of *HAD19* transcripts (lines 1, 8, and particularly 9) showed significantly abnormal leaves, as observed previously (Zhou et al., 2005). Two representative transgenic lines that constitutively expressed *HDA19* at elevated levels and contained a single T-DNA locus in their genomes, based on the ratio of antibiotic resistance phenotypes in progeny, were chosen for further study. Analysis of F3 homozygous plants from the two *HDA19*-overexpressing transgenic lines revealed little differences in growth, development, or morphology from wild-type plants. Following inoculation with *Pst*DC3000, the transgenic

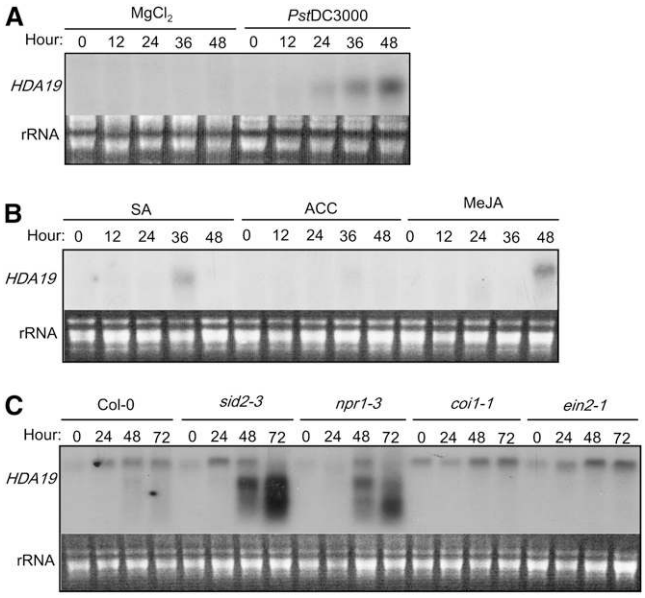

Figure 6. Expression of *HDA19*.

(A) Time course of pathogen-induced expression of *HDA19*. Five-week-old *Arabidopsis* plants (Col-0) were infiltrated with 10 mM $MgCl_2$ or *Pst*DC3000 (OD_{600} = 0.0001 in 10 mM $MgCl_2$). The infiltrated leaves were collected at the indicated times after inoculation for RNA isolation. RNA gel blot analysis was performed with a ^{32}P-labeled *HDA19* fragment.

(B) Time course of induced expression of *HDA19* by SA, 1-aminocyclopropane-1-carboxylic acid (ACC), and MeJA. Five-week-old *Arabidopsis* plants (Col-0) were sprayed with SA (1 mM), ACC (0.1 mM), and MeJA (0.1 mM). Leaf collection, RNA isolation, and RNA gel blot analysis of *HDA19* expression were performed as in **(A)**.

(C) Pathogen-induced expression of *HDA19* in defense signaling mutants. Five-week-old wild-type (Col-0), *sid2-3*, *npr1-3*, *coi1-1*, and *ein2-1* mutant plants were infiltrated with a suspension of *Pst*DC3000 (OD_{600} = 0.0001 in 10 mM $MgCl_2$). Leaf collection, RNA isolation, and RNA gel blot analysis of *HDA19* expression were performed as in **(A)**.

The experiments were performed three times with similar results.

HDA19 overexpression lines displayed substantially less bacterial growth (approximately fourfold to fivefold) than wild-type plants (Figure 7B). The inoculated leaves of *HDA19*-overexpressing plants also developed less severe disease symptoms than those of wild-type plants after infection (Figure 7D). These results support the notion that HDA19 has a positive role in basal resistance to the bacterial pathogen.

To investigate the molecular basis for the altered plant basal resistance against *Pst*DC3000, we analyzed *PR1* expression in the *hda19-3* mutant and *HDA19*-overexpressing transgenic plants after infection with the bacterial pathogen. After *Pst*DC3000 inoculation, the levels of *PR1* transcripts were reduced in the *hda19* mutant relative to those in the wild-type plants (Figure 7E). On the other hand, the levels of *PR1* transcripts in the *HDA19*-overexpressing plants were higher than those in wild-type plants, particularly at later stages of infection (i.e., at 48 and 72 HAI) (Figure 7F). These results suggest that HDA19 is a positive regulator of SA-regulated *PR1* gene expression.

Repression of Transcriptional Activation Activity of WRKY38 and WRKY62 by HDA19

Histone deacetylases catalyze the removal of acetyl groups from histone tails and often repress the transcription of genes by reducing the access of DNA by transcription factors (Zhou et al., 2005). Since HDA19 has a role in plant basal defense opposite to those of WRKY38 and WRKY62, it is possible that HDA19, through physical interaction, can reduce the transcriptional regulatory activity of the two transcription factors in plant cells. To test this possibility, we analyzed the transcriptional activation or repression activity of WRKY38 and WRKY62 using a transgenic system previously used for the analysis of WRKY7 (Kim et al., 2006). In this system, the transcriptional regulatory activity of a protein is determined through assays of a β-glucuronidase (*GUS*) reporter gene in stably transformed plants. The *GUS* reporter gene is driven by a synthetic promoter consisting of the −100 minimal *CaMV 35S* promoter and eight copies of the *LexA* operator sequence (see Supplemental Figure 8A online). Due to the minimal *35S* promoter used, these transgenic plants constitutively expressed low levels of the *GUS* reporter gene, thereby making them suitable for assays of transcription activation or repression by determining increases or decreases in GUS activities following coexpression of an effector protein.

To generate the WRKY38 and WRKY62 effectors, we fused their coding sequences with that of the DNA binding domain (DBD) of LexA. The fusion construct was subcloned behind the steroid-inducible *Gal4* promoter in pTA7002 (Aoyama and Chua, 1997) (see Supplemental Figure 8A online) and transformed into transgenic plants that already contain the *GUS* reporter construct. Unfused *WRKY38*, *WRKY62*, and *LexA DBD* genes were also subcloned into pTA7002 and transformed into transgenic *GUS* reporter plants as controls (see Supplemental Figure 8A online). Transgenic plants containing both the reporter and an effector construct were identified through antibiotic resistance screens. To determine how the effectors influence *GUS* reporter gene expression, we determined the changes of GUS activity in these transgenic plants following induction of the effector gene expression by spraying 20 μM dexamethasone (DEX), a steroid. In the transgenic plants that expressed the unfused *WRKY38*, *WRKY62*, or *LexA DBD* effector gene, the ratios of GUS activities measured before DEX treatment to those measured after DEX treatment were close to 1 (see Supplemental Figure 8B online). These results indicated that induced expression of *WRKY38*, *WRKY62*, or *LexA DBD* alone had no significant effect on expression of the *GUS* reporter gene. In the transgenic plants harboring the *LexA DBD-WRKY38* or *LexA DBD-WRKY62* effector gene, induction of the fusion effector after DEX treatment resulted in an approximately fourfold to sixfold increase in GUS activity (see Supplemental Figure 8B online). These results indicate that WRKY38 and WRKY62 are transcriptional activators in plant cells.

To determine how HDA19 affects the transcriptional activation activity of WRKY38 and WRKY62, we crossed the transgenic *35S:HDA19-L1* line with transgenic plants harboring both the *GUS* reporter and an effector gene. A transgenic line harboring an empty vector was also crossed with the transgenic reporter/effector double transformants as controls. As shown in Figure 8,

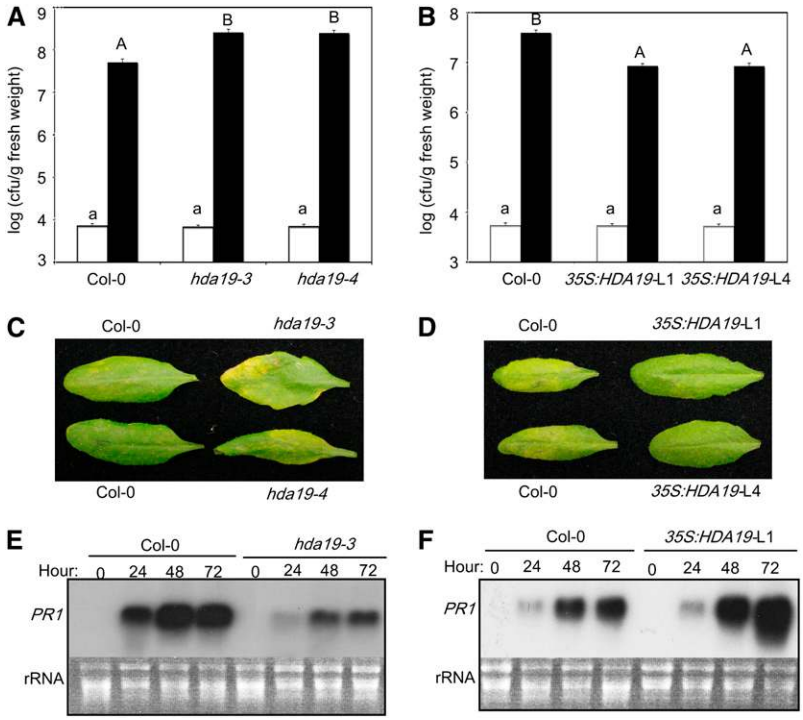

Figure 7. Altered Responses to *P. syringae* by the Mutant and Overexpression Plants for *HDA19*.

(A) and **(B)** Altered bacterial growth. The wild type (Col-0), *hda19* mutants **(A)**, and the overexpression lines **(B)** were infiltrated with a suspension of *Pst*DC3000 (OD_{600} = 0.0001 in 10 mM $MgCl_2$). Samples were taken at 0 (open bars) or 3 (closed bars) DAI to determine the growth of the bacterial pathogen. Means and SE were calculated from 10 plants for each treatment. According to Duncan's multiple range test (P = 0.05), means of colony-forming units do not differ significantly at 0 DAI if they are indicated with the same lowercase letter and do not differ significantly at 3 DAI if they are indicated with the same uppercase letter.

(C) and **(D)** Altered disease symptom development. Pathogen inoculation was performed as in **(A)** and **(B)**. Photographs of representative inoculated leaves to determine altered disease responses of the *hda19* mutants **(C)** were taken at 3 DAI. Photographs for the overexpression line **(D)** were taken at 4 DAI.

(E) and **(F)** Pathogen-induced *PR1* expression. Wild-type, *hda19*, and *HDA19*-overexpressing plants were infiltrated with a suspension of *Pst*DC3000 (OD_{600} = 0.0001 in 10 mM $MgCl_2$). Inoculated leaves were collected at the indicated times after inoculation for RNA isolation. RNA gel blot analysis was performed with ^{32}P-labeled *PR1*.

These experiments were performed four times with similar results.

in the progeny plants from the control cross with no constitutive *HDA19* overexpression, induced expression of the fused *LexA-WRKY38* or *LexA-WRKY62* effector gene after DEX treatment resulted in 3.5- to 6-fold induction in GUS activity, which was similar to that observed in their respective parental reporter/effector lines (see Supplemental Figure 8B online). On the other hand, in the progeny plants that constitutively overexpressed *HDA19*, induced expression of the fused *LexA-WRKY38* or *LexA-WRKY62* effector after DEX treatment resulted in no significant change in GUS activity (Figure 8). Thus, overexpressed HDA19 effectively abolished the transcriptional activation activity of WRKY38 and WRKY62.

To determine whether the histone deacetylase activity of overexpressed HDA19 is required to abolish the transcription activation activity of WRKY38 and WRKY62, we generated a mutant HDA19 (HDA19m) with Ala substitutions for His-148 and His-149, two evolutionarily invariant His residues located in a highly conserved motif of RPD3-type histone deacetylases, to which HDA19 belongs (see Supplemental Figure 9 online) (Kadosh and Struhl, 1998; Zhou et al., 2005). Ala substitutions for the two conserved His residues in RPD3-type histone deacetylases such as yeast RPD3 and Hos2 abolish their catalytic activity (Kadosh and Struhl, 1998; Sharma et al., 2007). When overexpressed in transgenic *Arabidopsis* plants, HDA19m was unable to alter plant growth or disease resistance (data not shown). However, HDA19m interacted with WRKY38 and WRKY62 based on BiFC (see Supplemental Figure 5 online) and coimmunoprecipitation assays (see Supplemental Figure 4B online). A transgenic *35S:HDA19m* line with the levels of *HDA19m* transcripts similar to those in the transgenic *35S:HDA19-L1* line was identified by RNA gel blotting and crossed with transgenic plants harboring both the *GUS* reporter and an effector gene. As shown in Figure 8, in the progeny plants that constitutively overexpressed *HDA19m*, induced expression of the fused *LexA-WRKY38* or *LexA-WRKY62* effector after DEX treatment resulted in 3.5- to 5-fold induction in GUS activity,

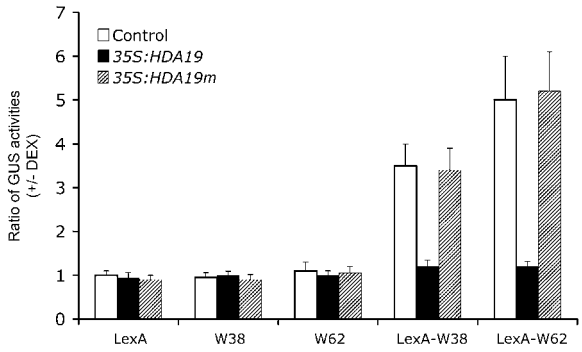

Figure 8. Antagonism of the Transcriptional Activation Activity of WRKY38 and WRKY62 by HDA19.

Effects of overexpressed HDA19 and HDA19m on the transcriptional activation activity of WRKY38 and WRKY62. The *HDA19*- or *HDA19m*-overexpressing line was crossed to lines harboring both the *GUS* reporter and one of the five tested effectors. A transgenic line containing an empty vector was also crossed to the same *GUS*/effector double transformants as controls. The ratios of GUS activities were calculated from the GUS activities determined in the leaves harvested 18 h after DEX treatment (+) over those determined prior to DEX treatment (−).

which was similar to that observed in their respective parental lines (Figure 8). Thus, overexpressed HDA19m did not abolish the transcription activation activity of WRKY38 and WRKY62.

To determine whether the ability of overexpressed HDA19 to abolish the transcription activation activity of a transcription factor is correlated with physical interaction, we examined the effect of overexpressed HDA19 on the transcription activation or repression activity of WRKY18 and WRKY48, which do not interact with HDA19 based on BiFC (see Supplemental Figure 5 online). However, induced expression of the *LexA DBD-WRKY18* effector gene had no significant effect on the GUS activity of the transgenic reporter/effector plants, indicating that WRKY18 has little transcription activation or repression activity in plant cells (data not shown). On the other hand, in the transgenic plants harboring the *LexA DBD-WRKY48* effector gene, induction of the fusion effector after DEX treatment resulted in an ~20-fold increase in GUS activity (see Supplemental Figure 10 online). This result indicated that WRKY48 is a strong transcription activator. The transgenic plants harboring both the *GUS* reporter and the *LexA DBD-WRKY48* effector gene was then crossed with the transgenic *35S:HDA19-L1* line. In the progeny plants that constitutively overexpressed *HDA19*, induced expression of the fused *LexA-WRKY48* after DEX treatment resulted in an ~20-fold induction in GUS activity, which was similar to that observed in the progeny derived from a cross with a control line transformed with an empty vector (see Supplemental Figure 10 online). Thus, overexpressed HDA19 did not significantly affect the transcription activation activity of WRKY48.

Functional Interaction of WRKY62 with HDA19 in Plant Disease Resistance

To analyze the functional interaction of the SA-regulated WRKY genes with *HDA19* in plant disease resistance, we examined the effects of overexpression of *WRKY62* on plant responses to *Pst*DC3000 in both the wild-type and *hda19* mutant backgrounds. The transgenic *35S:WRKY62-L1* line was crossed with the *hda19-3* mutant, and the *hda19-3/35S:WRKY62* plants in the F2 generation were identified by PCR and RNA gel blotting and compared with wild-type, *hda19-3* mutant, and *35S:WRKY62-L1* plants for responses to *Pst*DC3000. Following inoculation with the virulent bacterial pathogen, overexpression of *WRKY62* in the wild-type background (*35S:WRKY62-L1*) caused an approximately fivefold increase in bacterial growth (Figure 9A). Overexpression of *WRKY62* in the *hda19-3* mutant background (*hda19-3/35S:WRKY62-L1*), on the other hand, led to an ~15-fold increase in bacterial growth (Figure 9A). The inoculated leaves of the *hda19-3/35S:WRKY62-L1* plants also developed more severe disease symptoms than those of *hda19-3* and *35S:WRKY62-L1* plants after infection (Figure 9B). These results support the functional interaction of WRKY62 with HDA19 in plant disease resistance.

DISCUSSION

Negative Roles of WRKY38 and WRKY62 in Plant Defense

The *Arabidopsis NPR1* gene is an important regulator of plant disease resistance (Cao et al., 1997). Induced expression of

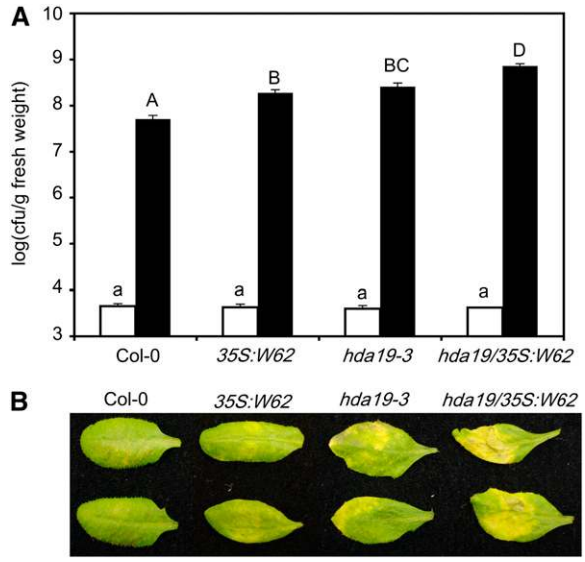

Figure 9. Altered Responses to *P. syringae* by Overexpression of *WRKY62* in the Wild-Type and *hda19* Mutant Backgrounds.

(A) Altered bacterial growth. Wild-type, *35S:WRKY62-L1*, *hda19-3*, and *hda19-3/35S:WRKY62* plants were infiltrated with a suspension of *Pst*DC3000 (OD_{600} = 0.0001 in 10 mM $MgCl_2$). Samples were taken at 0 (open bars) or 3 (closed bars) DAI to determine the growth of the bacterial pathogen. Means and SE were calculated from 10 plants for each treatment. According to Duncan's multiple range test (P = 0.05), means of colony-forming units at 0 DAI do not differ significantly if they are indicated with the same lowercase letter, and means of colony-forming units at 3 DAI do not differ significantly if they are indicated with the same uppercase letter.
(B) Altered disease symptom development. Pathogen inoculation was performed as in **(A)**. Photographs of representative inoculated leaves were taken at 3 DAI.

WRKY38 and *WRKY62* by pathogens, SA, and JA is dependent on NPR1 (Figure 1), suggesting that these two WRKY transcription factors function downstream of NPR1 in the regulation of plant defense responses. This interpretation is consistent with the recent finding that *WRKY38* is a direct target gene of NPR1 (Wang et al., 2006). In this study, we have demonstrated that disease resistance to *Pst*DC3000 is enhanced in the *wrky38* and *wrky62* single mutants and, to a greater extent, in the *wrky38 wrky62* double mutants (Figure 2). By contrast, overexpression of *WRKY38* or *WRKY62* reduces disease resistance (Figure 3). In addition, WRKY38 and WRKY62 suppress the expression of defense and defense-related genes, including SA-regulated *PR1* (Figures 3 and 4). These results indicate that WRKY38 and WRKY62 function additively as negative regulators of plant basal defense.

A large number of *Arabidopsis* WRKY genes are induced by infection with *Pst*DC3000, and a number of these pathogen-responsive WRKY genes have been analyzed for roles in plant basal disease resistance to the bacterial pathogen. Intriguingly, a majority of these functionally characterized pathogen-responsive WRKY genes function to repress plant basal resistance to the bacterial pathogen (Kim et al., 2006; Wang et al., 2006; Xu et al., 2006; Zheng et al., 2006, 2007; Shen et al., 2007). Some of the PAMP-induced WRKY negative regulators of plant defense have been proposed to provide a functional interface between PTI and ETI. For example, barley (*Hordeum vulgare*) WRKY1 and WRKY2 function as PAMP-inducible suppressors of basal defense (Shen et al., 2007). Upon avirulent effector recognition, barley MLA resistance protein can translocate to the nucleus and physically interact with the two WRKY proteins. The interactions apparently can interfere with the suppressor activity of the WRKY proteins, thereby derepressing PAMP-dependent basal defense during the activation of ETI (Shen et al., 2007). Possible inactivation of defense-suppressing WRKY proteins during ETI has also been proposed for *Arabidopsis* WRKY52/RRS1 R protein, which confers resistance toward the bacterial pathogen *Ralstonia solanacearum* (Eulgem and Somssich, 2007). A previous study has shown that the WRKY domain in WRKY52/RRS1 may play a negative role in defense signaling (Noutoshi et al., 2005). The interaction of RRS1 with its cognate effector PopP2 may inactivate the WRKY domain and activate high-amplitude defense mechanisms by derepression. Thus, during PTI, these defense-repressing WRKY proteins are induced by PAMP and may act to downregulate PAMP-induced plant defense responses so that they are not too deleterious to the host. During ETI, these defense-repressing WRKY proteins are inactivated upon functional recognition of avirulent factors by their cognate R proteins for derepression of defense mechanisms.

Both *Pst*DC3000 and SA induced *WRKY38* and *WRKY62* relatively quickly but transiently (Figure 1). The induction of the two negative regulators during the early stages of infection might serve as a mechanism to prevent unnecessary or even harmful overactivation of pathogen-induced defense mechanisms when the population of the pathogen is still at relatively low levels. As pathogen growth increases, enhanced defense mechanisms would be necessary, and this could be achieved at least partially by suppressed expression and inactivation of negative regulators such as WRKY38 and WRKY62. Indeed, the transcript levels of both *WRKY38* and *WRKY62* started to decline and eventually reached nearly basal levels between 12 and 24 h after pathogen infection (Figure 1). In addition, as the expression of *WRKY38* and *WRKY62* started to decrease, the transcript levels of *HDA19* started to increase concomitantly (Figure 6). The elevated HDA19 proteins from its induced expression would help to inactivate the remaining WRKY38 and WRKY62 transcriptional activators for a stronger defense response.

Pathogen-induced expression of negative defense regulators during plant defense responses could also be explained by their possible involvement in the antagonistic crosstalk of distinct signaling pathways against different types of microbial pathogens. SA-mediated signaling activates defense mechanisms effective against biotrophic pathogens but can suppress ET/JA-mediated signaling in defense against necrotrophic pathogens (Glazebrook, 2004). A WRKY protein that represses defense against one type of pathogen may function as an activator of defense against another type of microbial pathogen. For example, while its overexpression enhances susceptibility to biotrophic *Pst*DC3000, WRKY33 is an important positive regulator of plant resistance to necrotrophic fungal pathogens (Zheng et al., 2006). Although relatively resistant to *Pst*DC3000, the *wrky38* and *wrky62* mutants respond normally to the necrotrophic pathogens (data not shown). These results suggest that WRKY38 and WRKY62 do not play a major role in the antagonistic crosstalk of defense signaling pathways against these two types of pathogens. However, it is still possible that the two WRKY proteins play a positive role in plant responses to certain unknown abiotic or biotic stresses that may or may not be antagonized by SA- and NPR1-mediated defense.

Functional Antagonisms through Physical Interactions

Both defense-activating and defense-repressing WRKY proteins have been identified (Journot-Catalino et al., 2006; Kim et al., 2006; Li et al., 2006; Zheng et al., 2007), indicating that they are

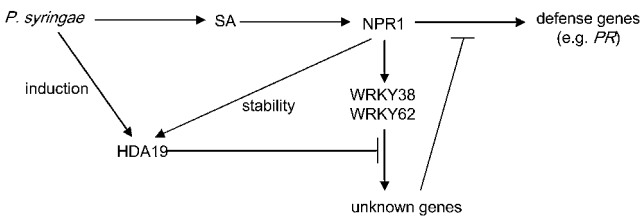

Figure 10. A Model for the Functional Interactions of WRKY38 and WRKY62 with HDA19 during Plant Defense Responses.

Infection by *P. syringae* leads to the accumulation of SA, which induces the expression of *WRKY38* and *WRKY62* in an NPR1-dependent manner. WRKY38 and WRKY62, as transcriptional activators, activate the expression of unknown regulatory genes that, in turn, repress the expression of defense genes (e.g., *PR1*) and basal disease resistance. Infection by *P. syringae* also induces *HDA19*, whose transcripts are stabilized by SA- and NPR1-mediated signaling. HDA19 represses the transcriptional activation activity of WRKY38 and WRKY62 and, as a result, reduces the activation of negative regulatory genes of plant basal defense by the two WRKY transcription factors.

critical regulators of differential and graded plant defense responses to distinct types of microbial pathogens. Understanding how these WRKY proteins interact functionally with each other and with other defense regulators will provide important insights into the molecular basis of the tight regulation and fine-tuning of plant defense responses. It has been proposed that the defense-repressing barley WRKY1 and WRKY2 can be inactivated by the interacting MLA R protein (Shen et al., 2007). Likewise, the interaction of *Arabidopsis* WRKY52/RRS1 with its cognate effector PopP2 has been suggested to inactivate the WRKY domain of RRS1 to activate high-amplitude defense mechanisms by derepression (Eulgem and Somssich, 2007). How the physical interaction leads to the inactivation of these WRKY proteins is unknown. In this study, we have demonstrated a simple mechanism by which the defense-repressing WRKY38 and WRKY62 can be inactivated by the interacting HDA19. Although WRKY38 and WRKY62 suppress disease resistance and repress defense gene expression, they act as transcriptional activators in plant cells (Figure 8). Thus, WRKY38 and WRKY62 do not appear to repress defense genes directly; more likely, they first activate certain unknown negative regulators that, in turn, repress defense genes (Figure 10). HDA19, on the other hand, is a positive regulator of plant basal resistance to *Pst*DC3000 (Figure 7). Histone deacetylases are often associated with transcriptional corepressor complexes by reducing histone acetylation levels to create repressed chromatin regions. Thus, one mode of action by HDA19 as a positive regulator of plant basal disease resistance is to counteract the WRKY38 and WRKY62 negative regulators of plant defense by binding directly to them and inactivating their transcriptional activation activity (Figure 10).

Regulation of Defense Responses by WRKY38/WRKY62 and HDA19

Both *WRKY38* and *WRKY62* are induced by SA and pathogens in an NPR1-dependent manner (Figure 1). Altered disease resistance in the *wrky38* and *wrky62* mutants and their overexpression lines was associated with altered expression of SA-regulated *PR1* gene expression (Figures 2 to 4). These results suggest that WRKY38 and WRKY62 are involved in SA signaling. *WRKY62* is also induced by JA (Mao et al., 2007). Likewise, HDA19 is induced by JA and plays an important role in JA-mediated defense responses (Zhou et al., 2005). Therefore, the functional interactions of WRKY38 and WRKY62 with HDA19 may be involved in both SA and JA signaling. SA and JA signaling pathways have a complicated relationship of interactions, including synergism and antagonism. A previous study has shown that synergism in the expression of JA-regulated genes (e.g., *PDF1.2* and *Thi2.1*) or SA-regulated genes (e.g., *PR1*) occurs when both signals are applied at low concentrations (Mur et al., 2006). However, when both signals are present at prolonged times or at high concentrations, antagonism between the two pathways is observed. In plants infected by *P. syringae*, JA signaling is activated weakly, as the JA-regulated genes were induced only at low levels (Glazebrook et al., 2003). However, this weakly activated JA signaling may synergistically interact with the activated SA signaling to augment plant defense against the invading bacterial pathogen. Pathogen- and JA-induced HDA19 may enhance SA signaling by inactivating negative SA signaling regulators such as WRKY38 and WRKY62.

The host-selective toxin HC-toxin produced by the filamentous fungus *Cochliobolus carbonum* is a critical determinant of virulence in the interaction with the host, maize (*Zea mays*) (Walton, 2006). HC-toxin inhibits maize histone deacetylases both in vitro and in vivo (Brosch et al., 1995; Ransom and Walton, 1997). It has been suggested that by inhibiting histone deacetylases, HC-toxin may interfere with the proper expression of a subset of plant host genes necessary for the host to mount an effective defense against the fungal pathogen (Ransom and Walton, 1997). Therefore, plant histone deacetylases might play a general role in maintaining the appropriate acetylation state of histones for proper induction of plant defense genes.

METHODS

Plant Growth Conditions

The *Arabidopsis thaliana* wild-type, mutant, and transgenic plants used in the study were all grown in growth chambers at 22°C and 120 $\mu E \cdot m^{-2} \cdot s^{-1}$ light on a 12-h-light/12-h-dark photoperiod.

Production of Recombinant Protein, and Electrophoretic Mobility Shift Assays

To generate the WRKY38 and WRKY62 recombinant proteins, their full-length cDNAs were cloned into pET32a (Novagen) and transformed into *Escherichia coli* strain BL21 (DE3). Induction of expression and purification of recombinant His-tagged proteins were performed according to the protocol provided by Novagen. The purified proteins were dialyzed overnight against a nuclear extraction buffer (25 mM HEPES/KOH, pH 7.5, 40 mM KCl, 0.1 mM EDTA, 10% glycerol, 1 mM DTT, and 30 μg/L phenylmethylsulfonyl fluoride) at 4°C. Double-stranded synthetic oligonucleotides were labeled to specific activities of $\sim 10^5$ cpm/ng using the Klenow fragment of DNA polymerase I. DNA and protein complexes were allowed to form at room temperature for 30 min and resolved on a 10% polyacrylamide gel in 0.5× Tris-borate-EDTA at 4°C.

Subcellular Localization

The *WRKY38* and *WRKY62* cDNAs were amplified and fused with the *GFP* gene in-frame in a pBluescript II SK vector. The empty GFP plasmid was used as a control. The plasmid was isolated using Qiagen kits, concentrated to ~1 μg/μL, and used to coat the gold particles for bombardment experiments. Transient expression of the *GFP* fusion genes in onion (*Allium cepa*) epidermal cells through particle bombardment and subsequent localization of the proteins were performed as described previously (Xu et al., 2006).

RNA Gel Blotting

For RNA gel blot analysis, total RNA (5 μg) was separated on agarose–formaldehyde gels and blotted to nylon membranes. Blots were hybridized with [α-^{32}P]dATP-labeled gene-specific probes. Hybridization was performed in PerfectHyb plus hybridization buffer (Sigma-Aldrich) overnight at 68°C. The membrane was then washed for 10 min twice with 2× SSC (1× SSC is 0.15 M NaCl and 0.015 M sodium citrate) and 1% SDS and for 10 min with 0.1× SSC and 1% SDS at 68°C. The probes used in RNA gel blotting were as follows: *WRKY38*, an ~450-nucleotide 3′ fragment obtained by *Xba*I/*Xho*I digestion of a full-length cDNA clone

isolated from a cDNA library (in ZAP Express λ vector from Stratagene) prepared from *Arabidopsis* plants harvested 4 h after spraying with 2 mM SA (Xu et al., 2006); *WRKY62*, an ~400-nucleotide 3′ fragment obtained by *Hin*dIII/*Xho*I digestion of a full-length cDNA clone; *HDA19*, a 747-nucleotide internal *Hin*dIII fragment from its full-length cDNA clone; and *PR1*, a 410-nucleotide PCR fragment amplified from the *Arabidopsis* genomic DNA using two *PR1*-specific primers (5′-TTCTTCCCTCGAAAG-CTCAA-3′ and 5′-CGTTCACATAATTCCCACGA-3′).

Quantitative RT-PCR

Total RNA was isolated from treated leaves and treated with DNA-free (Ambion) to remove contaminated genomic DNA. First-strand cDNA was synthesized with SuperScript II reverse transcriptase (Invitrogen) following the instructions of the manufacturer. Diluted first-strand cDNA was used as template, and real-time PCR was conducted with both ubiquitin primers (5′-GAAGGCGAAGATCCAAGACAAG-3′ and 5′-TCCCGGCGA-AAATCAATC-3′) and gene-specific primers (*WRKY38*, 5′-CGCCATGC-GGTTGAAGAG-3′ and 5′-TAACTTGAAAGCGGTCCACCAT-3′; *WRKY62*, 5′-CCAACCAGCTGCTCATCATG-3′ and 5′-GGCCAAATCCTCCCTT-TCC-3′; *HDA19*, 5′-GACTGTGATTACAACACACCGT-3′ and 5′-AATT-GCCGCCAGTATCCAT-3′). The PCR was set up using SYBR Green PCR Master Mix (Applied Biosystems) and run on the ABI Prism 7000 system. The relative specific mRNA abundance was calculated using ubiquitin as an internal control.

Isolation of Knockout Mutants

The *wrky38-1* (WiscDsLox489-492C21; in Col-0 ecotype) and *wrky38-2* (RATM11-6950-1_H; in No-0 ecotype) mutants each contain a *Ds* transposon in the second intron and the third exon of the *WRKY38* gene, respectively. Homozygous *wrky38* mutant plants were identified by PCR using a pair of primers corresponding to sequences flanking the *Ds* tagging sites (pW38F, 5′-ATGAACTCCCCACACGAAAAG-3′; pW38R, 5′-AAAGTAAAACTGATCATAACGATCCCA-3′). The *wrky62-1* (GABI_016H10; in Col-0 ecotype) and *wrky62-2* (RATM11-6212-1_G; in No-0 ecotype) mutants each contain a T-DNA insertion and a *Ds* transposon in the second exon of *WRKY62*. Homozygous *wrky62* mutant plants were identified by PCR using a pair of primers corresponding to sequences flanking the insertion sites (pW62F, 5′-ATGAACTCTTGCCAACAA-AAGGCT-3′; pW62R, 5′-TGATGATAAGTCGTGAGATGTCCA-3′). The *hda19-3* (SALK_139445) and *hda19-4* (SALK_139443) mutants each contain a T-DNA insertion in the first exon of the *HDA19* gene. Plants homozygous for the T-DNA insertions were identified by PCR using a pair of primers corresponding to sequence flanking the T-DNA insertion site (pHDA19F, 5′-CGCTCACTACGGTCTCCTTC-3′; pHDA19R, 5′-TAAA-GAACACGCTGCAAACG-3′). The *sid2-3* mutant (SALK_042603) contains a T-DNA insertion in the fourth intron of the *SID2* gene. Homozygous *sid2-3* mutant plants were identified by PCR using a pair of primers flanking the insertion site (pSID2F, 5′-TAGTTAGTGTGGCCATGCTAAG-3′; pSID2R, 5′-CCTAATTCCACGAGCCAAAA-3′).

Construction of *WRKY38*, *WRKY62*, and *HDA19* Overexpression Plants

An *Eco*RI/*Hin*dIII fragment that contains the *CaMV 35S* promoter with double enhancers, multiple cloning sites, and *35S* terminator was excised from pFF19 and cloned into the same sites of the transformation vector pOCA28 to generate pOCA30 (Chen and Chen, 2002). To generate the *35S:WRKY38* construct, the cDNA fragment that contains the full coding sequence and 3′ untranslated region of *WRKY38* was excised with *Sac*I and *Kpn*I from a cloning plasmid and subcloned into the same restriction sites of pOCA30 in the sense orientation behind the *35S* promoter. The *35S:WRKY62* construct was generated in a similar way by subcloning the full-length cDNA for *WRKY62* into the *Sma*I and *Xba*I sites of pOCA30. To generate the *35S:HDA19* construct, the cDNA fragment that contains the full coding sequence and 3′ untranslated region of *HDA19* was excised with *Spe*I and *Xho*I from a cloning plasmid and subcloned into the *Xba*I and *Sal*I sites of pOCA30 in the sense orientation behind the *35S* promoter. HDA19m with Ala substitutions for the catalytic His-148 and His-149 residues was generated by overlapping PCR and confirmed by sequencing. Briefly, two pairs of primers (pA408, 5′-ATCGAGCTCGTC-GACGTAATGGATACTGGCGGCAA-3′/pA409, 5′-TCGCACTTCTTAGC-GGCAGCGAGACCACCA-3′ and pA410, 5′-TGGTGGTCTCGCTGCC-GCTAAGAAGTGCGA-3′/pA411, 5′-AGCATAAAATGCCTCCTCCA-3′) were first used to amplify two DNA fragments from the full-length *HDA19* cDNA clone. The amplified two fragments were then used as templates for overlapping PCR using pA408 and pA411 as primers to amplify a DNA fragment of ~530 bp corresponding to the 5′ region of the *HDA19* coding sequence with introduced mutations. The fragment was digested with *Sac*I and used to replace the corresponding wild-type *Sac*I fragment of the full-length HDA19 cDNA clone.

Arabidopsis transformation was performed by the floral dip procedure (Clough and Bent, 1998). The seeds were collected from the infiltrated plants and selected in Murashige and Skoog medium containing 50 μg/mL kanamycin. Kanamycin-resistant plants were transferred to soil 9 d later and grown in a growth chamber for further analysis.

Pathogen Inoculation

Pathogen inoculations were performed by infiltration of leaves of at least six plants for each treatment with the *Pseudomonas syringae* pv *tomato* DC3000 strain (OD_{600} = 0.0001 in 10 mM $MgCl_2$). Inoculated leaves were harvested 3 d after infiltration and homogenized in 10 mM $MgCl_2$. Diluted leaf extracts were plated on King's B medium supplemented with rifampicin (100 μg/mL) and kanamycin (25 μg/mL) and incubated at 25°C for 2 d before counting the colony-forming units.

CytoTrap Two-Hybrid Screening

WRKY62-interacting proteins were identified using the CytoTrap two-hybrid system as described by the manufacturer (Stratagene). The *Arabidopsis* pMyr two-hybrid cDNA library was prepared from *Arabidopsis* plants harvested 4 h after spraying with 2 mM SA. The *WRKY62* cDNA was inserted into the *pSOS* plasmid to generate bait plasmids. The pMyr cDNA library and the corresponding bait plasmid were used to transform yeast strain cdc25H. Yeast transformants were plated onto the synthetic glucose minimal medium lacking uracil and Leu [SD/glucose(−UL)]. After growth at 25°C for 2 to 4 d, the colonies were replica-plated on the SD/galactose(−UL) plates and kept at 37°C. Those positive clones that grew on the SD/galactose(−UL) plates but not on the SD/glucose(−UL) plates were saved and analyzed further. Plasmid DNA was recovered from positive yeast colonies, transformed into *E. coli* strain DH5α, and isolated for DNA sequencing.

BiFC Assays

DNA sequences for the N-terminal 173–amino acid EYFP (N-YFP) and C-terminal 64–amino acid (C-YFP) fragments were PCR-amplified and cloned into the plant expression vectors pOCA30 (Chen and Chen, 2002) and pFGC5941 to generate pOCA-N-YFP and pFGC-C-YFP, respectively. The *WRKY18*, *WRKY38*, *WRKY62*, *WRKY48*, and *WRKY70* coding sequences were inserted into pOCA-N-YFP to generate the N-terminal in-frame fusions with N-YFP, whereas *HDA19* and *WRKY40* were introduced into pFGC-C-YFP to form C-terminal in-frame fusions with C-YFP. The resulting clones were verified through sequencing. The plasmids were introduced into *Agrobacterium tumefaciens* (strain GV3101), and infiltration of tobacco (*Nicotiana benthamiana*) was performed as described

previously (Cui et al., 2007). Infected tissues were analyzed at 16 to 24 h after infiltration. Fluorescence and DAPI staining were visualized by confocal microscopy using a Bio-Rad MRC-1024 laser scanning confocal imaging system.

Immunoprecipitation

To generate the FLAG- or MYC-tagged proteins, cDNA fragments for *WRKY38*, *WRKY62*, and *HDA19* were generated by PCR amplification and subsequently subcloned into a tagging plasmid behind the FLAG or MYC tag sequence as described previously (Xu et al., 2006). The tagged genes were subcloned into the plant transformation vector pOCA30, introduced into *A. tumefaciens* (strain GV3101), and infiltrated into tobacco as described previously (Cui et al., 2007). Preparation of protein extracts, immunoprecipitation, and detection of interacting proteins with protein gel blot analysis were performed as described previously (Xu et al., 2006).

Assays of Transcriptional Regulatory Activity of WRKY38 and WRKY62

Transgenic *Arabidopsis* plants containing a *GUS* reporter gene driven by a synthetic promoter consisting of the −100 minimal *CaMV 35S* promoter and eight copies of the *LexA* operator sequence were described previously (Kim et al., 2006). To generate effector genes, the DNA fragment for the LexA DBD was digested from the plasmid pEG202 (Clontech) using *Hin*dIII and *Eco*RI and cloned into the same sites in pBluescript. The full-length *WRKY18*, *WRKY38*, *WRKY48*, and *WRKY62* cDNA fragments were subsequently subcloned behind the *LexA DBD* to generate translational fusions. The *LexA DBD-WRKY* fusion genes were cloned into the *Xho*I and *Spe*I sites of pTA2002 behind the steroid-inducible promoter (Aoyama and Chua, 1997). As controls, the unfused *LexA DBD*, *WRKY38*, and *WRKY62* genes were also cloned into the same sites of pTA7002. These effector constructs were directly transformed into the transgenic GUS reporter plants, and double transformants were identified through screening for antibiotic (hygromycin) resistance. Determination of the activation or repression of *GUS* reporter gene expression by the effector proteins was performed as described previously (Kim et al., 2006).

Accession Numbers

Arabidopsis Genome Initiative numbers for the genes discussed in this article are as follows: *WRKY18*, At4g31800; *WRKY38*, At5g22570; *WRKY48*, At5g49520; *WRKY62*, At5g01900; *WRKY70*, At3g56400; *HDA19*, At4g38130; *PR1*, At2g14610; *NPR1*, At1g64280; *SID2*, At1g74710; *COI1*, At2g39940; *EIN2*, At5g03280.

Supplemental Data

The following materials are available in the online version of this article.

Supplemental Figure 1. Sequences, DNA Binding, and Subcellular Localization of WRKY38 and WRKY62.

Supplemental Figure 2. Analysis of the Expression of *WRKY38* (A) and *WRKY62* (B) by Quantitative RT-PCR.

Supplemental Figure 3. Loss-of-Function Mutants and Overexpression Lines for *WRKY38* and *WRKY62*.

Supplemental Figure 4. Determination of Protein–Protein Interactions by Yeast Two-Hybrid Assays and Coimmunoprecipitation.

Supplemental Figure 5. BiFC Analysis of Protein–Protein Interactions.

Supplemental Figure 6. Analysis of the Expression of *HDA19* by Quantitative RT-PCR.

Supplemental Figure 7. Generation and Characterization of Mutants and Overexpression Lines for *HDA19*.

Supplemental Figure 8. WRKY38 and WRKY62 Are Transcription Activators.

Supplemental Figure 9. Evolutionarily Invariant His Residues in a Highly Conserved Deacetylase Motif from *Arabidopsis* HDA19, Yeast Rpd3, and Hos2.

Supplemental Figure 10. Effect of the Transcription Activation Activity of WRKY48 by Overexpressed HDA19.

ACKNOWLEDGMENTS

We thank the ABRC at Ohio State University and the RIKEN Tsukuba Institute for the *Arabidopsis* mutants. We are grateful to Jixin Dong for his help with this work. This work was supported by National Science Foundation Grant MCB-0209819. This is journal paper 2007-18187 of the Purdue University Agricultural Research Program.

Received September 6, 2007; revised August 11, 2008; accepted August 18, 2008; published September 5, 2008.

REFERENCES

AbuQamar, S., Chen, X., Dhawan, R., Bluhm, B., Salmeron, J., Lam, S., Dietrich, R.A., and Mengiste, T. (2006). Expression profiling and mutant analysis reveals complex regulatory networks involved in *Arabidopsis* response to Botrytis infection. Plant J. **48:** 28–44.

Andreasson, E., et al. (2005). The MAP kinase substrate MKS1 is a regulator of plant defense responses. EMBO J. **24:** 2579–2589.

Aoyama, T., and Chua, N.-H. (1997). A glucocorticoid-mediated transcriptional induction system in transgenic plants. Plant J. **11:** 605–612.

Broder, Y.C., Katz, S., and Aronheim, A. (1998). The ras recruitment system, a novel approach to the study of protein-protein interactions. Curr. Biol. **8:** 1121–1124.

Brosch, G., Ransom, R., Lechner, T., Walton, J.D., and Loidl, P. (1995). Inhibition of maize histone deacetylases by HC toxin, the host-selective toxin of *Cochliobolus carbonum*. Plant Cell **7:** 1941–1950.

Cao, H., Glazebrook, J., Clarke, J.D., Volko, S., and Dong, X. (1997). The *Arabidopsis* NPR1 gene that controls systemic acquired resistance encodes a novel protein containing ankyrin repeats. Cell **88:** 57–63.

Chen, C., and Chen, Z. (2000). Isolation and characterization of two pathogen- and salicylic acid-induced genes encoding WRKY DNA-binding proteins from tobacco. Plant Mol. Biol. **42:** 387–396.

Chen, C., and Chen, Z. (2002). Potentiation of developmentally regulated plant defense response by AtWRKY18, a pathogen-induced Arabidopsis transcription factor. Plant Physiol. **129:** 706–716.

Clough, S.J., and Bent, A.F. (1998). Floral dip: A simplified method for *Agrobacterium*-mediated transformation of *Arabidopsis thaliana*. Plant J. **16:** 735–743.

Cui, X., Fan, B., Scholz, J., and Chen, Z. (2007). Roles of *Arabidopsis* cyclin-dependent kinase C complexes in cauliflower mosaic virus infection, plant growth, and development. Plant Cell **19:** 1388–1402.

Dong, J., Chen, C., and Chen, Z. (2003). Expression profile of the *Arabidopsis* WRKY gene superfamily during plant defense response. Plant Mol. Biol. **51:** 21–37.

Eulgem, T., Rushton, P.J., Robatzek, S., and Somssich, I.E. (2000). The WRKY superfamily of plant transcription factors. Trends Plant Sci. **5:** 199–206.

Eulgem, T., and Somssich, I.E. (2007). Networks of WRKY transcription factors in defense signaling. Curr. Opin. Plant Biol. **10:** 366–371.

Glazebrook, J. (2004). Contrasting mechanisms of defense against biotrophic and necrotrophic pathogens. Annu. Rev. Phytopathol. **43:** 205–227.

Glazebrook, J., Chen, W., Estes, B., Chang, H.S., Nawrath, C., Metraux, J.P., Zhu, T., and Katagiri, F. (2003). Topology of the network integrating salicylate and jasmonate signal transduction derived from global expression phenotyping. Plant J. **34:** 217–228.

Jones, J.D., and Dangl, J.L. (2006). The plant immune system. Nature **444:** 323–329.

Journot-Catalino, N., Somssich, I.E., Roby, D., and Kroj, T. (2006). The transcription factors WRKY11 and WRKY17 act as negative regulators of basal resistance in *Arabidopsis thaliana*. Plant Cell **18:** 3289–3302.

Kadosh, D., and Struhl, K. (1998). Histone deacetylase activity of Rpd3 is important for transcriptional repression in vivo. Genes Dev. **12:** 797–805.

Kalde, M., Barth, M., Somssich, I.E., and Lippok, B. (2003). Members of the *Arabidopsis* WRKY group III transcription factors are part of different plant defense signaling pathways. Mol. Plant Microbe Interact. **16:** 295–305.

Kim, K.C., Fan, B., and Chen, Z. (2006). Pathogen-induced Arabidopsis WRKY7 is a transcriptional repressor and enhances plant susceptibility to *Pseudomonas syringae*. Plant Physiol. **142:** 1180–1192.

Kloek, A.P., Verbsky, M.L., Sharma, S.B., Schoelz, J.E., Vogel, J., Klessig, D.F., and Kunkel, B.N. (2001). Resistance to *Pseudomonas syringae* conferred by an *Arabidopsis thaliana* coronatine-insensitive (coi1) mutation occurs through two distinct mechanisms. Plant J. **26:** 509–522.

Knoth, C., Ringler, J., Dangl, J.L., and Eulgem, T. (2007). *Arabidopsis* WRKY70 is required for full RPP4-mediated disease resistance and basal defense against *Hyaloperonospora parasitica*. Mol. Plant Microbe Interact. **20:** 120–128.

Kunkel, B.N., and Brooks, D.M. (2002). Cross talk between signaling pathways in pathogen defense. Curr. Opin. Plant Biol. **5:** 325–331.

Li, J., Brader, G., Kariola, T., and Palva, E.T. (2006). WRKY70 modulates the selection of signaling pathways in plant defense. Plant J. **46:** 477–491.

Li, J., Brader, G., and Palva, E.T. (2004). The WRKY70 transcription factor: A node of convergence for jasmonate-mediated and salicylate-mediated signals in plant defense. Plant Cell **16:** 319–331.

Long, J.A., Ohno, C., Smith, Z.R., and Meyerowitz, E.M. (2006). TOPLESS regulates apical embryonic fate in *Arabidopsis*. Science **312:** 1520–1523.

Mao, P., Duan, M., Wei, C., and Li, Y. (2007). WRKY62 transcription factor acts downstream of cytosolic NPR1 and negatively regulates jasmonate-responsive gene expression. Plant Cell Physiol. **48:** 833–842.

Mur, L.A., Kenton, P., Atzorn, R., Miersch, O., and Wasternack, C. (2006). The outcomes of concentration-specific interactions between salicylate and jasmonate signaling include synergy, antagonism, and oxidative stress leading to cell death. Plant Physiol. **140:** 249–262.

Noutoshi, Y., Ito, T., Seki, M., Nakashita, H., Yoshida, S., Marco, Y., Shirasu, K., and Shinozaki, K. (2005). A single amino acid insertion in the WRKY domain of the *Arabidopsis* TIR-NBS-LRR-WRKY-type disease resistance protein SLH1 (sensitive to low humidity 1) causes activation of defense responses and hypersensitive cell death. Plant J. **43:** 873–888.

Park, C.Y., Lee, J.H., Yoo, J.H., Moon, B.C., Choi, M.S., Kang, Y.H., Lee, S.M., Kim, H.S., Kang, K.Y., Chung, W.S., Lim, C.O., and Cho, M.J. (2005). WRKY group IId transcription factors interact with calmodulin. FEBS Lett. **579:** 1545–1550.

Petersen, M., et al. (2000). *Arabidopsis* MAP kinase 4 negatively regulates systemic acquired resistance. Cell **103:** 1111–1120.

Ransom, R.F., and Walton, J.D. (1997). Histone hyperacetylation in maize in response to treatment with HC-toxin or infection by the filamentous fungus *Cochliobolus carbonum*. Plant Physiol. **115:** 1021–1027.

Rushton, P.J., Torres, J.T., Parniske, M., Wernert, P., Hahlbrock, K., and Somssich, I.E. (1996). Interaction of elicitor-induced DNA-binding proteins with elicitor response elements in the promoters of parsley PR1 genes. EMBO J. **15:** 5690–5700.

Sharma, V.M., Tomar, R.S., Dempsey, A.E., and Reese, J.C. (2007). Histone deacetylases RPD3 and HOS2 regulate the transcriptional activation of DNA damage-inducible genes. Mol. Cell. Biol. **27:** 3199–3210.

Shen, Q.H., Saijo, Y., Mauch, S., Biskup, C., Bieri, S., Keller, B., Seki, H., Ulker, B., Somssich, I.E., and Schulze-Lefert, P. (2007). Nuclear activity of MLA immune receptors links isolate-specific and basal disease-resistance responses. Science **315:** 1098–1103.

Spoel, S.H., et al. (2003). NPR1 modulates cross-talk between salicylate- and jasmonate-dependent defense pathways through a novel function in the cytosol. Plant Cell **15:** 760–770.

Tian, L., and Chen, Z.J. (2001). Blocking histone deacetylation in *Arabidopsis* induces pleiotropic effects on plant gene regulation and development. Proc. Natl. Acad. Sci. USA **98:** 200–205.

Tian, L., Wang, J., Fong, M.P., Chen, M., Cao, H., Gelvin, S.B., and Chen, Z.J. (2003). Genetic control of developmental changes induced by disruption of *Arabidopsis* histone deacetylase 1 (AtHD1) expression. Genetics **165:** 399–409.

Ulker, B., and Somssich, I.E. (2004). WRKY transcription factors: From DNA binding towards biological function. Curr. Opin. Plant Biol. **7:** 491–498.

Walton, J.D. (2006). HC-toxin. Phytochemistry **67:** 1406–1413.

Wang, D., Amornsiripanitch, N., and Dong, X. (2006). A genomic approach to identify regulatory nodes in the transcriptional network of systemic acquired resistance in plants. PLoS Pathog. **2:** e123.

Wildermuth, M.C., Dewdney, J., Wu, G., and Ausubel, F.M. (2001). Isochorismate synthase is required to synthesize salicylic acid for plant defence. Nature **414:** 562–565.

Xu, X., Chen, C., Fan, B., and Chen, Z. (2006). Physical and functional interactions between pathogen-induced *Arabidopsis* WRKY18, WRKY40, and WRKY60 transcription factors. Plant Cell **18:** 1310–1326.

Yu, D., Chen, C., and Chen, Z. (2001). Evidence for an important role of WRKY DNA binding proteins in the regulation of NPR1 gene expression. Plant Cell **13:** 1527–1540.

Zheng, Z., Mosher, S.L., Fan, B., Klessig, D.F., and Chen, Z. (2007). Functional analysis of *Arabidopsis* WRKY25 transcription factors in plant defense against *Pseudomonas syringae*. BMC Plant Biol. **7:** 2.

Zheng, Z., Qamar, S.A., Chen, Z., and Mengiste, T. (2006). *Arabidopsis* WRKY33 transcription factor is required for resistance to necrotrophic fungal pathogens. Plant J. **48:** 592–605.

Zhou, C., Zhang, L., Duan, J., Miki, B., and Wu, K. (2005). HISTONE DEACETYLASE19 is involved in jasmonic acid and ethylene signaling of pathogen response in *Arabidopsis*. Plant Cell **17:** 1196–1204.